Metamaterials and the Control of Electromagnetic Fields

JB Pendry
The Blackett Lab
Imperial College London
London SW7 2AZ
UK
j.pendry@imperial.ac.uk

Abstract: A new class of materials, metamaterials, whose properties are engineered by controlling their nanostructure, open new vistas in optics and offer the possibility of lenses that can resolve details finer than the wavelength of light.
©2007 Optical Society of America
OCIS codes: (160.0160) Materials; (999.9999) metamaterials & negative refraction

1. Metamaterials – what are they?

Conventional materials owe their properties to the individual atoms and molecules from which they are composed. The macroscopic electromagnetic fields are averages over the fluctuating local fields, averages that are very well defined as there are typically billions of molecules contained in one cubic wavelength of matter. Metamaterials extend this concept replacing the molecules with man made structures that might have dimensions of nanometers for visible light or in the case of GHz radiation may be as large as a few millimeters, but still much less than the wavelength. In this way properties are engineered through *structure* rather than through *chemical composition*. Fig. 1 illustrates this concept.

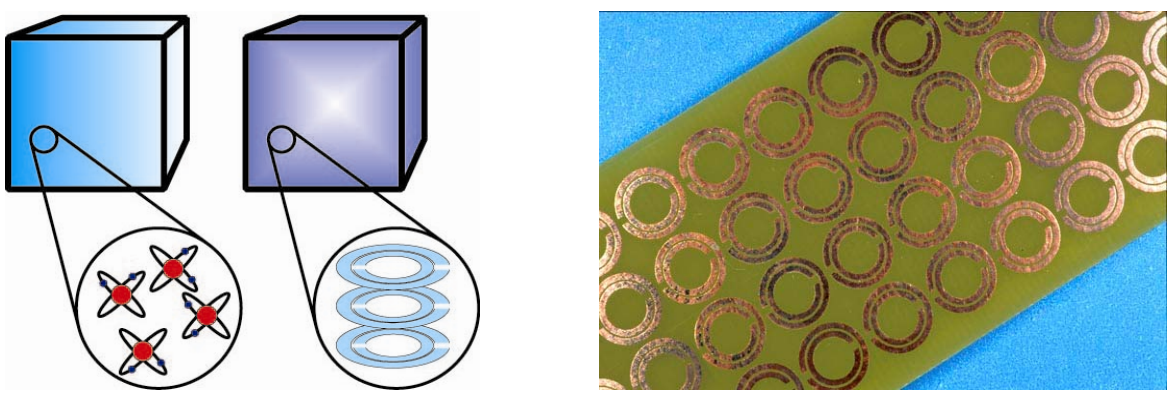

Fig. 1. Left: in conventional materials ε, μ derive from the constituent atoms; in metamaterials $\varepsilon_{eff}, \mu_{eff}$ derive from the sub-units which may contain many atoms. Right: an early example of a metamaterial with a resonant magnetic response. Split rings are etched onto a copper circuit board. Dimensions of a few millimeters give a resonant frequency of around 10GHz.

An early example of a metamaterial designed to give a magnetic response is shown to the left of fig. 1 [1]. Other structures giving novel electrical responses have also been reported. [2].

Metamaterials are particularly valuable for use in controlling the near field. Structured on a scale much less than the wavelength the near field can peer into the microstructure of a material. Ultimately the most detailed near fields will detect the individual units from which a material is made and at this point a description in terms of $\varepsilon_{eff}, \mu_{eff}$ must fail. If we wish to use our metamaterials in a near field context, for example to build a superlens and achieve sub wavelength resolution, the structural units must be designed to be smaller than the length scales of the fields.

Another class of artificial material deriving its properties from structure is the *photonic* crystal [3]. In contrast to metamaterials, photonic crystals deploy structures having roughly the same size as the wavelength since their properties derive from diffraction of radiation. In general photonic crystals have a complex response to electromagnetic radiation that is too rich to be described by a simple $\varepsilon_{eff}, \mu_{eff}$. For some photonic crystals a simple description in terms of $\varepsilon_{eff}, \mu_{eff}$ is possible but only on length scales down to the lattice spacing. Therefore,

valuable as photonic crystals may be in some applications, they are not useful in near field experiments which probe sub-wavelength details of the structure.

The additional design flexibility given by the structural dimension of metamaterials enables properties to be realized that have never before been observed. These properties can easily be made anisotropic and made to vary as a function of position. New possibilities are opened by these materials and hence the great interest that they have aroused.

The sort of structure deployed varies according to purpose. Perhaps the most common structures so far have been resonant elements. Resonances have the characteristic that their response reverses as the frequency tunes through the resonance and hence have been used to produce negative magnetic responses as is the case for the structure shown in Fig. 1, or negative electrical response if conducting wires are used. Negative magnetic and negative electric responses taken together fulfill the long sought after Veselago prescription for a negative refractive index [4] and have opened a whole new field of research to experiment that is proving fruitful of new theoretical concepts and has the potential for valuable applications.

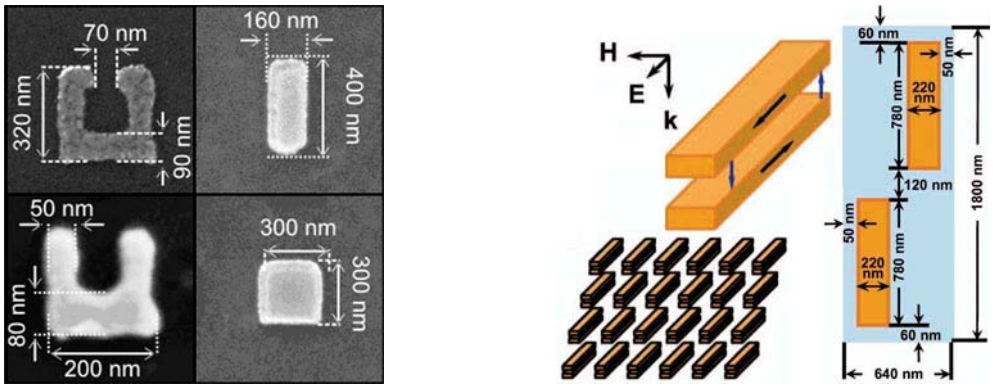

Fig. 2. Magnetism at near optical frequencies. Left: Elements of a magnetic metamaterial manufactured using ebeam lithography by the Wegener group [5] to work in the range 100-300THz. Right: a design from the Shalaev group [6] combining a magnetic and electrical resonance in the same structure through the symmetric and antisymmetric resonances of a pair of gold bars.

Progress in metamaterials has been rapid. One theme has been to extend the frequency range from the microwave region where the first tests were made up towards optical frequencies. The relatively crude etching of split rings on copper circuit boards has been replaced with sophisticated lithographic techniques reducing dimensions to nanometers rather than millimeters. Thus metamaterials magnetically active first at THz frequencies have been reported and more recently in the near infrared [5] deploying miniaturized refinements of the original split ring. See fig. 2. Another instance of high frequency structures is shown on the right of fig. 2. This shows a design by the Shalaev group based on a unit of two parallel gold bars. The bars support two resonances: a symmetric electrically active mode and an antisymmetric magnetically active one. Tuning the parameters so that the resonances coincide in frequency results in a metamaterial exhibiting negative refraction.

Fig. 3. Left: Element of a chiral metamaterial designed to work at a wavelength of around 10m with extreme chirality [7]. Right: realization of this structure by Mike Wiltshire

Some groups have designed metamaterials to work in the MHz region of the spectrum with magnetic resonance imaging as the target application. Resonances at such low frequencies require high capacitance and inductance realized in the 'Swiss roll' structure shown in fig. 3. The particular structure shown is designed to be chiral and comprises an insulated gold tape wound at an angle around a cylinder to form a helix. In contrast to most other chiral systems this particular design exhibits an extreme chiral response: the plane of polarization can be rotated by $90°$ within one wavelength of propagation. By way of comparison even highly concentrated sugar solutions require propagation over 10^3 wavelengths to achieve the same rotation.

Not all metamaterials contain resonant elements. Generally speaking, if negative values of ε or μ are required, then it is essential to have a resonant element in the metamaterial. Fig. 4 shows a non resonant design for anisotropic diamagnetism at the ultimate low frequency: DC. It is a challenge to make anisotropic materials that are diamagnetic at zero frequency such as may be required for cloaking of magnetic fields as we shall discuss later in this paper. However superconductors allow the necessary persistent currents to flow and these can be designed to act against the applied field and hence yield diamagnetism.

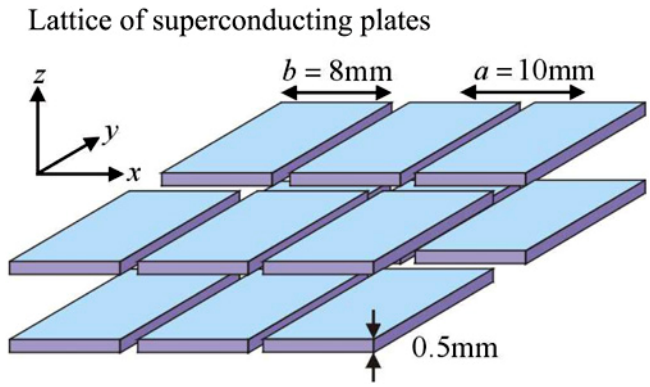

Fig. 4. A metamaterial designed to give anisotropic magnetism at DC [8]. A magnetic field acting in the *z*- direction has to squeeze between the superconducting plates giving rise to diamagnetism. Fields acting in the *x*- and *y*- directions are unaffected by the thin plates.

Table 1. Effective medium parameters for superconducting plates shown in fig. 4. Lattice constant $a = 10\text{mm}$ ($a \times a \times a$ cubic lattice)

$b(\text{mm})$	$\mu_x = \mu_y$	$\varepsilon_x = \varepsilon_y$	μ_z
8.0	1.00	1.84	0.74
9.5	1.00	3.45	0.47
9.8	1.00	5.47	0.32

Despite the great amount of creative activity surrounding metamaterials much remains to be done. This is especially true at the optical end of the spectrum. Here the most promising structures comprise metal/dielectric layers, particularly those involving silver: the metal supplies a negative permittivity to complement the positive permittivity of the dielectric. By adjusting the ratio of metal to dielectric and tuning the frequency a wide variety of anisotropic properties can be obtained. however the layers are generally required to be extremely flat. Asperities on the metal as small as a few nanometers attract a large density of surface plasmon states which act as a sink for radiation and therefore constitute a loss process.

Loss is a serious issue when metamaterials are used in sub-wavelength applications. These generally work through resonant features of the spectrum and are therefore vulnerable to loss. Even silver, although the best performing noble metal in this respect, is far from ideal. The restrahlen bands of ionic materials such as silicon carbide perform far better in this respect, but their application is confined to the far infra red. Silicon carbide does however have the advantage that it can be deposited using conventional semiconductor growth technology and therefore the interfaces are of a much higher quality than those of metals. Little has been done to search for other negative permittivity materials with low losses. In particular it might be profitable to explore experimentally the alloy system of CsAu which is an ionic insulator but comprises two metals each with long lived plasmon excitations.

At GHz frequencies losses are much less of an issue and it is mainly the dielectric component of the structure that is lossy. The longer length scales mean that much more complex structures become feasible with current

technology, though an issue that will need to be addressed is the development of cheap and efficient manufacturing processes capable of handling 3D structures. Currently structures are manufactured in 2D panels and assembled into 3D structures by cottage industry techniques (i.e. graduate students). This will need to change before mass application of metamaterial technology comes on stream.

At low frequencies, MHz down to DC, much less work has been done possibly because the structures required are more complex even than the GHz structures and hence more time consuming to manufacture: compare fig. 1 to fig. 3. Yet there is much potential in this range. Conventional ferromagnets are heavy and prone to loss and hysteresis but metamaterials usually consist mainly of air and are therefore light. The absence of any intrinsic magnetism in the components removes hysteresis and much of the loss.

2. Negative refraction

It was undoubtedly the concept of negative refraction that brought metamaterials to prominence. Seriously studied for the first time by Veselago [4] negative refraction is achieved when at the same frequency,

$$\varepsilon(\omega) < 0, \qquad \mu(\omega) < 0 \tag{1}$$

Using Maxwell's equations to calculate the refractive index gives,

$$n = \pm\sqrt{\varepsilon\mu} \tag{2}$$

and conventional materials take the positive sign. Veselago showed that, if condition (1) is met, the negative sign for n is the one that satisfies causality. The many fascinating properties explored in the Veselago paper attracted much interest at the time but the subject resisted all experimental attempts due to the complete absence of any naturally occurring negatively refracting materials. In time interest died away and the paper was largely forgotten until the first PECS conference at Laguna beach in 1999 where I reported [1] our first attempts at designing electric and magnetic metamaterials. David Smith and Shelly Schultz were enthusiastic about the new materials and went on to manufacture the first negatively refracting substance every made by combining a negative permittivity and a negative permeability metamaterial in the same structure [9, 10]. Their work fired a huge amount of interest, not all of it positive, but the validity of their conclusions has now been confirmed many times over. Their paper opened the way for experimental exploration of Veselago's theoretical concepts.

It is worth asking why scientists and engineers are so intrigued by negative refraction. After all positive refraction is well understood so why should a sign flip add special interest? A clue is found in the refraction process itself. Consider fig. 5. The requirements that energy flow *normal* to the surface and wave vector *parallel* to the surface are incompatible in the presence of negative refraction unless the energy flow is opposite to the wave vector.

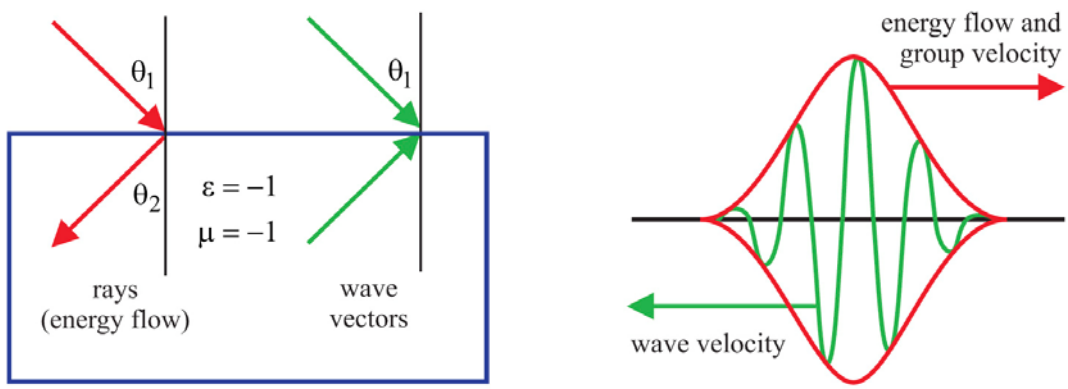

Fig. 5. Left: in a double negative material as described by Veselago, light makes a negative angle with the normal. Note that the parallel component of the wave vector is always preserved in transmission, but that energy flow is opposite to the wave vector. Right: by implication the wave velocity and the Poynting vector have opposite signs.

The mathematical implications of this statement are that the refractive index must disperse strongly with frequency. Taking the definitions of the wave and group velocities,

$$v_w = c_0/n, \qquad v_g = d\omega/dk = c_0/\left(n + \omega\, dn/d\omega\right) \tag{3}$$

Requiring that v_w and v_g have opposite signs we deduce,

$$\omega\, dn/d\omega > |n| \tag{4}$$

where we have assumed n to be negative. Let us choose a frequency ω_2 at which $n(\omega_2) < 0$ then by integrating (4),

$$\ln(n_2/n_1) > -\ln(\omega_2/\omega_1), \qquad \omega_2 > \omega_1 \tag{5}$$

and hence,

$$|n_1| > |n_2|\omega_2/\omega_1 \tag{6}$$

Therefore as ω_1 heads down in frequency n_1 becomes more and more negative. At some point there is a divergence, $n_1 \to -\infty$. In practice we run into limitations on the validity of the metamaterial concept: if n_1 becomes so large that the wavelength is comparable to the size of the metamaterial elements, then the refractive index is no longer a valid concept and there is a cut off. If the metamaterial is a period structure the cut off will occur at the Brillouin zone boundary in $k-$ space and we can easily count the resonances: there will be twice as many as there are cells in the structure. We have counted one resonance for each transverse polarization state. There will also be magnetic and electric longitudinal states which we shall not discuss here.

This divergence of the refractive index at some frequency is an essential feature of negative refraction. It also implies that negative refracting materials have a very high density of states. The essential components of a negatively refracting metamaterial are the local resonances comprising the units from which the material is assembled. We require two resonances per cell and typically one of these will be magnetic in character and the other electrical.

Perhaps the most exciting aspect of negative fraction is the ability to interact strongly with the near field, a quality brought about by the internal resonances discussed above. The most remarkable discovery was that negative refraction enables a prescription to be given for a perfect lens, capable of reproducing an image in every detail unlimited by wavelength provided only that the prescription is met exactly. Veselago had already predicting focusing of rays of light as shown in fig. 6. However much later [11] it was realized that this Veselago lens also focuses the near field under the conditions,

$$\varepsilon \to -1, \qquad \mu \to -1\text{, and hence } n \to -1 \tag{7}$$

In so far as these two conditions are met, the image is perfect in every detail, and there are no spurious reflections at the surface of the lens.

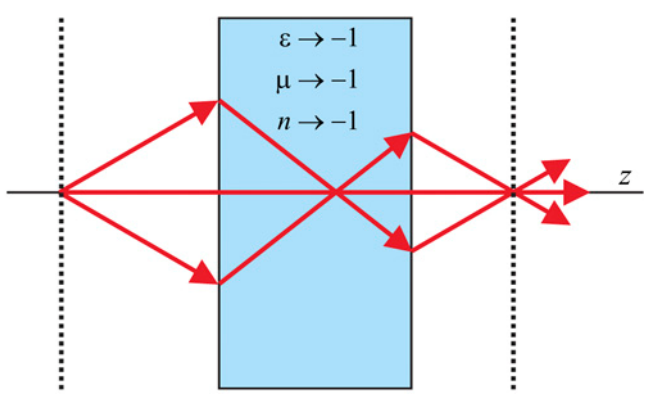

Fig. 6. A negative refractive index medium bends light to a negative angle relative to the surface normal. Light formerly diverging from a point source in the object plane is set in reverse and converges back to a point. Released from the medium the light reaches a focus for a second time in the image plane.

This is a remarkable result because, in order to 'focus' the near field, amplification has to take place to compensate for the natural decay and furthermore the amplification has to be exactly tuned to each Fourier

component of the field. Surfaces of negatively refracting materials are heavily decorated with resonant states under the conditions specified by (7) these states are almost degenerate at nearly the same frequency and amplification takes place by stimulation of these resonances. It is a relatively slow process of course and very specific to the frequency at which (7) is obeyed.

Sub wavelength focusing was first realized by the Eleftheriades group at GHz frequencies [12] where the necessary metamaterials are available. However an optical version of the lens is much more difficult. Although metals such as silver have an intrinsic permittivity that is negative, magnetic responses at optical frequencies are rare and as yet we do not have a fully 3D negatively refracting optical material at least not one that is capable of sub wavelength operation.

An approximation to the perfect lens can be had if all the dimensions are much less that the wavelength. Under these conditions the electric and magnetic components of the field are almost independent and we are free to concentrate on the electrical part ignoring magnetic effects. A purely electrical field is indifferent to μ and therefore it should be possible to construct a 'poor man's lens' of silver by tuning the frequency so that $\varepsilon \approx -1$. Losses in the silver prevent exact realization of this condition but nevertheless a version of this poor man's lens was built by the Xiang group in Berkeley [13], and by the Blakie group in Canterbury New Zealand [14, 15]. They demonstrated sub wavelength imaging on a scale of a few tens of nanometers. More recently silver has been replaced by silicon carbide where the low loss restrahlen bands give a much better approximation to $\varepsilon \approx -1$ and hence better resolution as a fraction of the wavelength. A resolution of $\lambda/20$ was achieved in the silicon carbide experiment shown in fig. 7 [16].

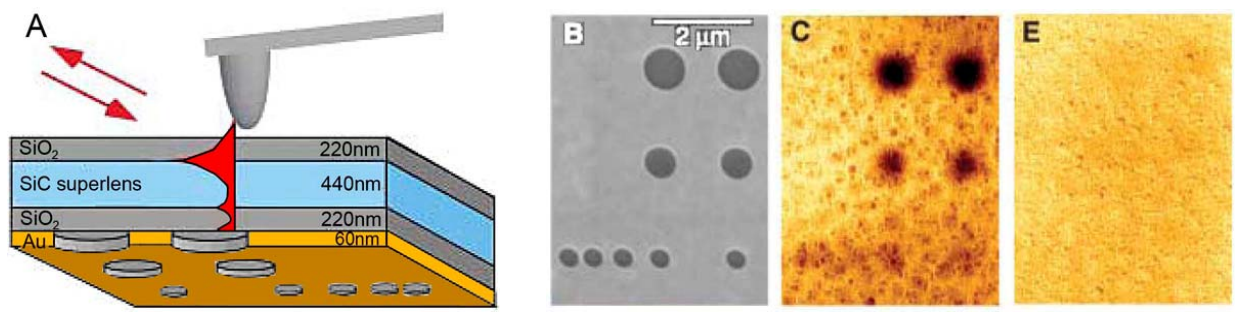

Fig. 7. A: a silicon carbide superlens is sandwiched between two layers of dielectric. Light incident on a scanning probe tip scatters and is focused on the gold layer below where it reflects from details of the structure inscribed in the gold. The lens refocuses this scattered light on the tip where it scatters a third time before reaching a detector. B: SEM image of the gold layer; C: images at a frequency where $\varepsilon \approx -1$ showing a resolution of up to $\lambda/20$. E: the lens is detuned to a different frequency violating the conditions for perfect lensing and no images are seen.

3. Transformation Optics

Metamaterials give enormous choice of material parameters for electromagnetic applications. So much so that we might ask if there is a new way to design electromagnetic systems exploiting this new flexibility. In an ideal world magnetic and electrical field lines can be placed anywhere that the laws of physics allow and a suitable metamaterial found to accommodate the desired configuration of fields. It was to answer the question of what parameters to choose for the metamaterial that we developed transformation optics [17, 18, 19, 20]. The idea is quite straightforward: start with a field pattern that obeys Maxwell's equations for a system that is topologically similar to the desired configuration but confined either to free space or a simple configuration of permittivity and permeability, then distort the system until the fields are in the desired configuration. If we imagine that the original system was embedded in an elastic matrix in which Cartesian coordinate lines were drawn, then after distortion the deformed coordinates could be described by a coordinate transformation. Next rewrite Maxwell's equations using the new coordinate system. Some time ago it was shown that Maxwell's equation are of the same form in any coordinate system but the precise values of permittivity and permeability will change. These new values of permittivity and permeability are the ones we must give to our metamaterial if we want the fields to take up the distorted configuration.

Although the prescription is simple enough it is very powerful in what can be achieved. For example: the Veselago lens shown in fig. 6 suffers from the limitation that the image is exactly the same size as the object. Our new design methodology easily remedies this limitation: imagine a coordinate system that is stretched in the region of the image thus stretching the image. Transformation optics then prescribes the metamaterials with which this can be achieved [18]. Or consider the lens itself. Focusing can be thought of in general terms as a distortion of space in

which the coordinate system is folded back on itself so that we see the same set of trajectories three times as the three layers of folded space overlap. Applying this description and calculating the metamaterial properties gives rise to the configuration shown in fig. 6. Less esoteric applications might employ metamaterials to collect and concentrate light onto a solar cell.

To give a flavor of how the scheme operates imagine the simplest possible distortion of space: a section of the $x-$ axis is compressed as shown in fig. 8. We probe the compressed region with two rays in order to find the values of $\boldsymbol{\varepsilon}(\mathbf{r})$ and $\boldsymbol{\mu}(\mathbf{r})$ that would give rise to the ray trajectory shown. We recognize that:

- $\boldsymbol{\varepsilon}(\mathbf{r}), \boldsymbol{\mu}(\mathbf{r})$ are tensors because we have singled out the *x*-axis for compression,
- in the uncompressed regions there is no change so $\boldsymbol{\varepsilon}(\mathbf{r}) = \boldsymbol{\mu}(\mathbf{r}) = 1$ in these regions,
- $\boldsymbol{\varepsilon}(\mathbf{r})$ and $\boldsymbol{\mu}(\mathbf{r})$ appear on the same footing because of the symmetry between electric and magnetic fields.

It follows from the last assertion that $\boldsymbol{\varepsilon}(\mathbf{r}) = \boldsymbol{\mu}(\mathbf{r})$.

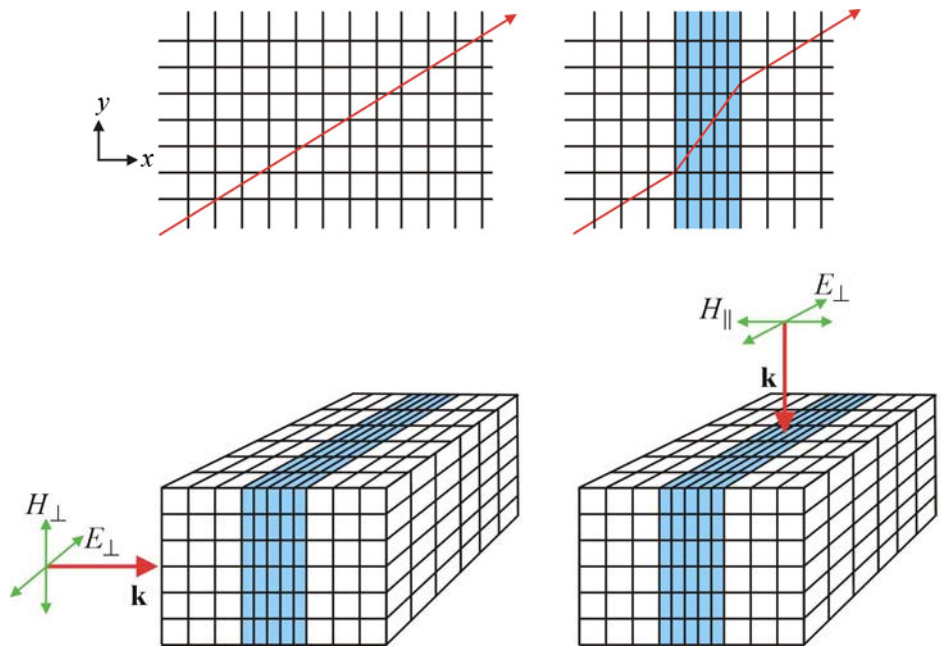

Fig. 8. Top: a simple coordinate transformation than compresses a section of the $x-$ axis. As a result rays follow a distorted trajectory shown on the top right but emerge from the compressed region traveling in exactly the same direction with the same phase as before. Bottom: requiring that a ray pass through the compressed region with the same phase change as through uncompressed space enables us to predict the metamaterial properties that would realize this trajectory for a ray.

Next consider a ray propagating parallel to the $x-$axis: in order to arrive at the far side of the compressed region with the same phase as in the uncompressed system we require $k'md = k_0 d$ where k_0 is the free space wave vector, k' is the wave vector in the compressed region, m is the compression factor, and d is the original thickness of the layer. Since $k' = k_0\sqrt{\varepsilon_y \mu_y}$, where ε_y and μ_y are the components of the respective tensors perpendicular to the $x-$axis, then we deduce that,

$$\varepsilon_y = \mu_y = m^{-1} \tag{8}$$

On the other hand rays propagating perpendicular to the $x-$axis travel through uncompressed space, and therefore their wave vector, k'', must take the free space value if the correct phase evolution is to be followed. In this case,

$$k'' = k_0\sqrt{\varepsilon_y \mu_x} = k_0\sqrt{\varepsilon_x \mu_y} = k_0 \tag{9}$$

and therefore using (8) we have,

$$\varepsilon_x = \mu_x = m \tag{10}$$

Also: because $\boldsymbol{\varepsilon}(\mathbf{r}) = \boldsymbol{\mu}(\mathbf{r})$, the compressed layer is impedance matched and does not reflect.

The above gives an intuitive version of our scheme. A more formal derivation was presented by Ward and Pendry [18] and an updated version by Schurig et al [19] using modern notation [20]. We follow the latter version here. If the distorted system is described by a coordinate transform $x'^{j'}\left(x^j\right)$ we define,

$$\Lambda_j^{j'} = \frac{\partial x^{j'}}{\partial x^j} \tag{11}$$

Then in the new coordinate system we must use modified values of the permittivity and permeability to ensure that Maxwell's equations are satisfied,

$$\begin{aligned} \varepsilon'^{i'j'} &= \left[\det(\Lambda)\right]^{-1} \Lambda_i^{i'} \Lambda_j^{j'} \varepsilon^{ij} \\ \mu'^{i'j'} &= \left[\det(\Lambda)\right]^{-1} \Lambda_i^{i'} \Lambda_j^{j'} \mu^{ij} \end{aligned} \tag{12}$$

As a challenge for transformation optics we set the problem of constructing a cloak of invisibility. Two problems confront us: first we must eliminate scattered radiation and hence no radiation must reach the hidden object; second the hidden object must cast no shadow. The latter is the more difficult of the two to achieve. Several solutions have been proposed in the literature [21, 22, 23, 24], our solution [21] is to construct a cloak that guides radiation around the hidden space but allowing to resume its original course on the far side. An observer would see the same radiation as if neither the cloak nor the hidden object were present. One advantage of our scheme is that any object can be placed inside the cloak and still remain hidden.

Our starting point is free space and we confine our cloak to a sphere of radius R_2. Next we select an infinitely small sphere at the centre of the big sphere. Infinitely small spheres are always invisible whatever they are made of. Next we expand the infinitesimal sphere into a finite sphere radius $R_1 < R_2$. As we expand the infinitesimal sphere we imagine that all the field lines and coordinate lines are compressed into the annulus between R_1 and R_2. Outside the larger sphere nothing is disturbed. There are several coordinate transformations that achieve this result. We pick a simple one here given in spherical polar coordinates:

$$r' = \frac{R_2 - R_1}{R_2} r + R_1, \qquad \theta' = \theta, \qquad \phi' = \phi \tag{13}$$

Equation (12) then gives,

$$\begin{aligned} \varepsilon'^{r'} &= \mu'^{r'} = \frac{R_2}{R_2 - R_1}\left[\frac{(r' - R_1)}{r'}\right]^2, \qquad R_1 > r' > R_2 \\ \varepsilon'^{\theta'} &= \mu'^{\theta'} = \varepsilon'^{\phi'} = \mu'^{\phi'} = \frac{R_2}{R_2 - R_1} \end{aligned} \tag{14}$$

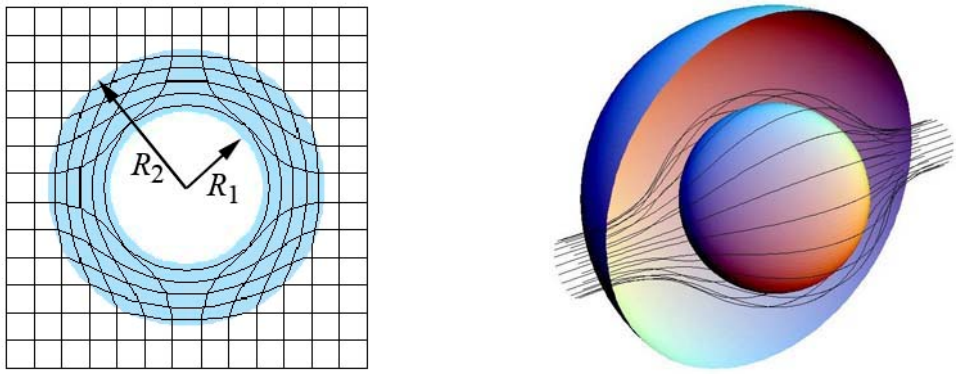

Fig. 9. Left: a schematic of the coordinate transformation presented in equation (13). Right: trajectories of rays through the cloak showing how they avoid the cloaked region and return to their original path after traversing the cloak.

Deploying these values of permittivity and permeability enables radiation to be guided around the hidden space as illustrated in fig. 9. The effectiveness of the cloak has been demonstrated first by computer simulations and more recently by an experimental realization [25].

There are three topologically distinct routes to a cloak. In the scheme presented above we started from an infinitesimal sphere and expanded it into a finite sphere within which we can hide objects. If we consider the inverse transformation, $x^j\left(x'^{j'}\right)$, then viewed from the outside the cloaked region *appears* to contain empty space with a infinitesimal sphere at the centre containing the crushed contents of the cloak. Inverting the transformation results in very large values of permittivity and permeability for the crushed objects. However they still remain invisible: even a perfectly conducting sphere will vanish in the limit of infinitesimal radius.

Next consider the case where instead of spheres we work with cylinders. The principle is the same: a cloak contained between an outer and inner cylinder. From outside the cloak we shall see a region of empty space and at its centre an cylinder of infinitesimal radius. In general we can expect the crushing process to give this cylinder or wire a very large conductivity. It might be thought that an thin conducting wire would still be visible but in fact this is not the case: if the wire is extremely thin it will have large inductance preventing any current from being induced in the wire. So the cylindrical cloak is still theoretically perfect.

Lastly consider the case where instead of crushing the hidden volume to an infinitesimal sphere, or to a wire of infinitesimal radius, we crush to an infinitesimally thin plate. In general this will appear to have very high conductivity and of course now we cannot get away with claiming a perfect cloak because a conducting sheet is definitely visible! However the transformations concerned have the virtue of being non- singular unlike equation (14) and therefore may have some value for cloaking in situations where we can hide the infinitesimally thin plate on an infinitely conducting ground plane.

Transformation optics can also be used to give another interpretation the Veselago lens shown in fig. 6. The lens exists in a coordinate system x, y, z but viewed from outside it would appear as though the region between the object plane and the image plane vanishes. This can be expressed as a coordinate transformation,

$$\begin{aligned} &x' = x, \quad y' = y', \\ &z' = z, \qquad\qquad z < z_1, \\ &z' = \left(2z_1 - z\right), \quad z_1 < z < z_1 + d, \\ &z' = z - 2d, \quad z_1 + d < z \end{aligned} \tag{15}$$

where the lens is assumed lies in the range $z_1 < z < z_1 + d$ where the x, y, z space maps on to a triple valued x', y', z' space. Applying the transformation formulae (11) and (12) gives,

$$\begin{aligned} &\varepsilon = \mu = +1, \qquad z < z_1, \\ &\varepsilon = \mu = -1, \quad z_1 < z < z_1 + d, \\ &\varepsilon = \mu = +1, \quad z_1 + d < z \end{aligned} \tag{16}$$

Now we can give a geometrical interpretation to the lens: it comprises a section of ‘negative’ space that annihilates an equivalent thickness of vacuum.

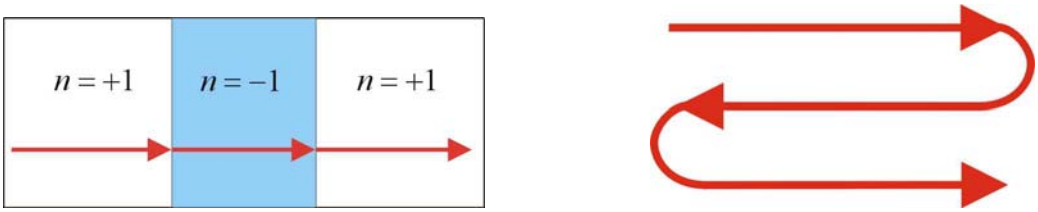

Fig. 10. Left: in the x, y, z coordinate system space is single valued and a ray progresses continuously through the region of negative refraction. Right: an equally legitimate view point is that the refractive index is everywhere positive but space is triple valued, doubling back on itself so that each point within the range of the lens is crossed thrice.

There is a close analogy between the transformed ε, μ and the metric of a space and it may be that this can in the future be exploited to realize, at least in an optical sense, some esoteric geometries.

4. Conclusions

Metamaterials and the new fields of research they have spawned are relatively recent arrivals on the scene: not even ten years old. And yet such is the activity that this review is a rather breathless one only touching on the many facets of the subject [26, 27]. Those of us working on metamaterials are excited by the intellectual stimulation of this new perspective on an old subject. We are constantly surprised by the sometimes controversial conclusions we are forced to and stimulated by the realization that exoteric theory can have experimental realization. The latter will, I am sure, lead the way to applications. Indeed there are already many patents held on metamaterials, a sign that I am not alone in this expectation. Who knows what directions this lively field will take in the next decade.

4. references

[1] J. B. Pendry, A. J. Holden, D. J. Robbins and W. J. Stewart, *IEEE Trans. Micr. Theory and Techniques*, **47**, 2075 (1999).

[2] J. B. Pendry, A. J. Holden, W. J. Stewart, I. Youngs, *Phys. Rev. Lett.*, **76**, 4773 (1996).

[3] M. Notomi, Phys. Rev. B62, 10696 (2000).

[4] V. G. Veselago, *Soviet Physics USPEKI* 10, 509 (1968).

[5] S. Linden, C. Enkirch, M. Wegener, J. Zhou, T. Koschny & C, M, Soukoulis, Magnetic response of metamaterials at 100 THz, *Science* **306**, 1351 (2004); T.J. Yen, W.J. Padilla, N. Fang, D.C. Vier, D.R. Smith, J.B. Pendry, D.N. Basov, X. Zhang *Science*, **303** 1494-1496 (2004); G. Dolling, M. Wegener, C.M. Soukoulis, S. Linden, *Optics Letters* **32** 53-55 (2007).

[6] Vladimir M. Shalaev, Wenshan Cai, Uday K. Chettiar, Hsiao-Kuan Yuan, Andrey K. Sarychev, Vladimir P. Drachev, and Alexander V. Kildishev *Optics Letters* **30** 3356 (2005)

[7] J.B. Pendry *Science* **306** 1353-5 (2004)

[8] B. Wood & J.B. Pendry *Phys. Rev.* **B74** 115116 (2006).

[9] D. R. Smith, W. J. Padilla, D. C. Vier, S. C. Nemat-Nasser, S. Schultz, *Phys. Rev. Lett.*, 84, 4184 (2000).

[10] R. A. Shelby, D. R. Smith, S. Schultz, *Science* 292, 77 (2001).

[11] J.B. Pendry *Phys. Rev. Lett.* **85,** 3966-9 (2000).

[12] A. Grbic, G. V. Eleftheriades, *Phys. Rev. Lett.*, 92, 117403 (2004).

[13] N. Fang, H. Lee, C. Sun and X. Zhang *Science* **308** 534 (2005)

[14] R.J. Blaikie and D.O.S Melville *J. Opt. A: Pure Appl. Opt.* **7** S176 (2005).

[15] D.O.S.Melville and R.J. Blaikie *Opt. Express* **13** 2127 (2005).

[16] T. Taubner, D. Korobkin, Y. Urzhumov, et al. *Science* **313** 1595-1595 (2006).

[17] A. J. Ward and J. B. Pendry, *Journal of Modern Optics*, 43 773 (1996).

[18] J.B. Pendry and S.A. Ramakrishna, *J. Phys.: Condens. Matter* **15** 6345–6364, (2003).

[19] D. Schurig, J.B. Pendry, D.R. Smith *Optics Express*, **14**, Issue 21, 9794-9804 (2006).

[20] D.M. Shyroki http://arxiv.org/abs/physics/0307029v1 (2003)

[21] J.B. Pendry, D. Schurig, and D.R. Smith *Science* **312** 1780-2 (2006).

[22] U. Leonhardt, *Science* **312**, 1777 (2006).

[23] A. Alu, N. Engheta, *Phys. Rev.* E95, 016623 (2005).

[24] G. W. Milton, N.-A. P. Nicorovici, *Proc. Roy. Soc. London A* **462**, 1364 (2006).

[25] D. Schurig, J. J. Mock, B. J. Justice, S. A. Cummer, J. B. Pendry, A. F. Starr, D. R. Smith *Science*, **314,** 977-80 (2006).

[26] J.B. Pendry, *Contemporary Physics* **45** 191-202 (2004).

[27] D.R. Smith, J.B. Pendry, M.C.K. Wiltshire, *Science* **305** 788-92 (2004).